

The Hybrid Organic-Inorganic 2-D Material (CsNa₂[{Sn(CH₃)₂(H₂O)₄(β-XW₉O₃₃)]·7H₂O)_∞ (X = As^{III}, Sb^{III}) and Its Solution Properties^[‡]

Firasat Hussain,^[a] Markus Reicke,^[a] and Ulrich Kortz^{*[a]}

Keywords: Hybrid materials / Organometallic compounds / Polyoxometalates / Self assembly / Tungsten

We report on the hybrid organic-inorganic 2-D materials (CsNa₂[{Sn(CH₃)₂(H₂O)₄(β-AsW₉O₃₃)]·7H₂O)_∞ (**1a**) and the isomorphous (CsNa₂[{Sn(CH₃)₂(H₂O)₄(β-SbW₉O₃₃)]·7H₂O)_∞ (**2a**) which crystallize in the orthorhombic system, space group *Pna*2₁, with identical unit cell parameters *a* = 26.118(2) Å, *b* = 16.064(1) Å, *c* = 13.776(1) Å, and *Z* = 1. Compounds **1a** and **2a** have been synthesized in good yield by crystallization from a reaction mixture of dimethyltin dichloride and Na₉[α-XW₉O₃₃] (X = As^{III}, Sb^{III}) in aqueous, acidic medium. We have shown by multinuclear NMR spectroscopy (¹⁸³W, ¹¹⁹Sn, ¹³C, ¹H) that **1a** and **2a** decompose in solution

leading to the monomeric species [{Sn(CH₃)₂(H₂O)₂]₃(β-XW₉O₃₃)]³⁻ [X = As^{III} (**1**), Sb^{III} (**2**)]. Polyanions **1** and **2** consist of a (β-XW₉O₃₃) fragment stabilized by three dimethyltin units. The dimethyltin groups are grafted onto the polyanion by two Sn–O(W) bonds on the side of the heteroatom lone pair. Compounds **1** and **2** are rare examples of discrete polyoxoanions which polymerize upon crystallization leading to a 2-D solid-state structure with inorganic and organic surface regions.

(© Wiley-VCH Verlag GmbH & Co. KGaA, 69451 Weinheim, Germany, 2004)

Introduction

Polyoxometalates are of interest because they exhibit a tremendous structural variety and useful properties in different fields, including catalysis and medicine.^[1–6] This is most likely the reason why the number of researchers actively involved in polyoxoanion chemistry has increased significantly over the last couple of decades. A study of the literature reveals that the vast majority of reports is devoted to catalytic studies of polyoxoanion salts and acids.

Most likely this is a result of the fact that the synthesis of novel polyoxoanion architectures is not trivial. Although the template effect seems to play an important role during the formation process of polyoxoanions, the detailed mechanism of formation is far from being understood. This is even more surprising as the first polyoxoanions were reported almost two centuries ago.^[7] However, it took another 100 years for the first structure (the Keggin ion) to be determined.^[8]

It is known that the size, shape and charge density of many polyoxoanions are of interest for pharmaceutical applications (e.g. antiviral, antitumor).^[1–6,9] However, the mechanism of action of many polyoxoanions is not selective towards a specific target. In order to improve selectivity it

often appears desirable to modify a given polyoxoanion core structure slightly. However, such attempts result frequently in a different polyoxoanion framework. Therefore the most straightforward and promising approach towards systematic derivatization of polyoxoanions involves attachment of organic groups to the surface of the metal-oxo framework. In order to be attractive for pharmaceutical applications the functionalized polyoxoanions should be water soluble and fairly stable at physiological pH.

To date the number of water-soluble polyoxoanions with tightly bound organic functions is rather small. Pope and co-workers were the first to study the interaction of monoorganotin groups with polyoxoanions. They reacted different organotin halide precursors (e.g. *n*C₄H₉SnCl₃, C₆H₅SnCl₃) with a large number of lacunary heteropolytungstates in aqueous solution and were able to identify novel, mostly dimeric polyoxoanion structures.^[10] Single-crystal X-ray diffraction studies revealed that these products contain tightly anchored organotin fragments. The compounds were also studied in solution by multinuclear NMR spectroscopy. This technique is also very valuable in the evaluation of the stability of polyoxoanions in low concentration at physiological pH for medicinal applications. Liu and co-workers have also synthesized some monoorganotin-substituted polyoxotungstates. They introduced ester functionalities to the organotin fragment and tested the biological (antitumor) activity of their products.^[11] Very recently Hasenknopf et al. used the same methodology to introduce peptide functions into organotin units which were incorporated in the monolacunary Wells–Dawson deriva-

[‡] Polyoxoanions Functionalized by Diorganotin Groups, Part 1.

[a] International University Bremen, School of Engineering and Science

P. O. Box 750 561, 28725 Bremen, Germany

Fax: (internat.) + 49-(0)421-200-3229

E-mail: u.kortz@iu-bremen.de

tive $[\alpha\text{-P}_2\text{W}_{17}\text{O}_{61}]^{10-}$ ($x = \alpha_1, \alpha_2$).^[12] Haiduc et al. have also reported some monoorganotin derivatives of polyoxotungstates.^[13] However, the proposed structures of Liu and Haiduc need to be confirmed by X-ray diffraction. To date, only a few monoorganotin-substituted polyoxomolybdates and -vanadates are known.^[14]

Interestingly there are no reports on diorganotin-substituted polyoxotungstates. Such species could allow for more flexibility regarding the interaction with, and binding to, organic compounds and biomolecules. Therefore we decided to investigate the interaction of dimethyltin groups with lone-pair-containing heteropolytungstates in some detail.

Results and Discussion

Here we report on the novel and isostructural polyoxoanion-based 2-D materials $(\text{CsNa}_2[\{\text{Sn}(\text{CH}_3)_2\}_3(\text{H}_2\text{O})_4(\beta\text{-XW}_9\text{O}_{33})]\cdot 7\text{H}_2\text{O})_\infty$ ($\text{X} = \text{As}$, **1a**; Sb , **2a**; see Figure 1). The structure of **1a** and **2a** is best described as a polymeric network composed of $[\{\text{Sn}(\text{CH}_3)_2\}_3(\text{H}_2\text{O})_4(\beta\text{-XW}_9\text{O}_{33})]^{3-}$ building blocks ($\text{X} = \text{As}^{\text{III}}$, Sb^{III}) that are linked by $\text{Sn}-\text{O}(\text{W}')$ bridges. This leads to a 2-D surface which is not planar, but could be described as a ladder with a zig-zag backbone where the individual levels are decorated by methyl groups (see Figure 2). Clearly, the solid-state structure of **1a** and **2a** is governed by the organotin functionalities.

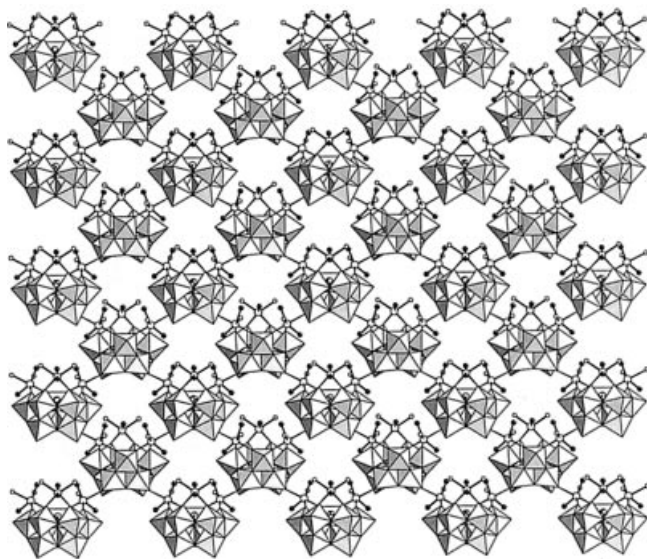


Figure 1. Combined polyhedral/ball-and-stick representation of the 2-D solid-state structure of $(\text{CsNa}_2[\{\text{Sn}(\text{CH}_3)_2\}_3(\text{H}_2\text{O})_4(\beta\text{-XW}_9\text{O}_{33})]\cdot 7\text{H}_2\text{O})_\infty$ ($\text{X} = \text{As}$, **1a**; Sb , **2a**); the octahedra represent WO_6 and the balls are tin (diagonally hatched), arsenic/antimony (crosshatched), oxygen (white) and carbon (black); hydrogen atoms are omitted for clarity

Compounds **1a** and **2a** are isostructural, which means that the different sizes of the As and Sb heteroatoms with their associated lone pairs have no significant effect on the solid-state structures.



Figure 2. Side view of the 2-D solid-state structure of **1a** and **2a**; the code is the same as in Figure 1

The three organotin groups attached to each monomeric unit of **1a** and **2a** contain tin centers that are octahedrally coordinated by four oxo and two methyl groups which are positioned *trans* to each other. However, only two organotin groups are structurally equivalent and different from the third. The molecular formulae and charges of **1a** and **2a** are supported by bond-valence calculations, which indicate that all terminal oxygen atoms bound to the tin atoms are diprotonated.^[15]

Close inspection of **1a** and **2a** indicates that the $\text{C}-\text{Sn}-\text{C}$ bond angles are significantly smaller than 180° , indicating that the interior methyl groups still experience some degree of repulsion (see Figure 1). The $\text{C}-\text{Sn}-\text{C}$ bond angles of the two equivalent organotin groups are very similar for **1a** [$149(1)^\circ$, $152(1)^\circ$] and **2a** [$150(1)^\circ$, $151(1)^\circ$]; however, the $\text{C}-\text{Sn}-\text{C}$ bond angle of the unique organotin unit is distinctly larger in polyanion **1a** [$166(1)^\circ$] than in **2a** [$162(1)^\circ$]. This observation reflects (a) the smaller size of the As^{III} atom compared to Sb^{III} , (b) the shorter $\text{As}^{\text{III}}-\text{O}$ bond lengths compared to Sb^{III} , and (c) the smaller size of the As^{III} lone-pair compared to Sb^{III} .

It is known that the α to β isomerization of $[\alpha\text{-AsW}_9\text{O}_{33}]^{9-}$ and $[\alpha\text{-SbW}_9\text{O}_{33}]^{9-}$ is facilitated in an acidic, aqueous medium.^[16,17] This is in complete agreement with the synthetic conditions for **1a** and **2a**, which were isolated at pH 3. The $(\beta\text{-AsW}_9\text{O}_{33})$ fragment has so far only been observed in two different polyoxoanion structures.^[16,18] The large tungstoarsenate(III) $[\text{As}_6\text{W}_{65}\text{O}_{217}(\text{H}_2\text{O})_7]^{26-}$ is the only example of a polyanion that contains both $(\alpha\text{-AsW}_9\text{O}_{33})$ and $(\beta\text{-AsW}_9\text{O}_{33})$ isomers in the same structure.^[18]

The fact that no cations are involved in the exclusively covalent 2-D network of **1a** and **2a** requires it to possess a negative charge. Indeed the appropriate number of cations (1 Cs, 2 Na) for each polyanionic unit was found by X-ray diffraction and elemental analysis. Therefore **1a** and **2a** are best described as polymeric polyanion salts. This view is further supported by our observation that **1a** and **2a** are soluble in water upon heating.

Clearly, in solution the polymeric structure of **1a** and **2a** decomposes and we identified the likely sites: the very long Sn–O(W') bonds in **1a** [2.607(3), 2.656(3) Å] and **2a** [2.559(3), 2.633(3) Å]. The question now arises in which form **1a** and **2a** are present in solution: oligomeric or monomeric. The latter requires the existence of the hypothetical, monomeric polyanion $[\{\text{Sn}(\text{CH}_3)_2(\text{H}_2\text{O})_2\}_3(\beta\text{-XW}_9\text{O}_{33})]^{3-}$ [X = As^{III} (**1**), Sb^{III} (**2**)]. Polyanion **1** consists of a (β -AsW₉O₃₃) fragment which is stabilized by three dimethyltin fragments, and polyanion **2** represents its antimony derivative (see Figures 3 and 4). The three dimethyltin groups of **1** and **2** are grafted onto the polyanion by two Sn–O(W) bonds each on the side of the heteroatom lone pair.

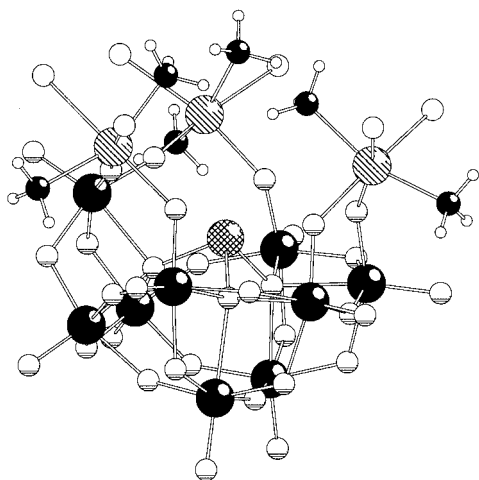


Figure 3. Ball-and-stick representation of $[\{\text{Sn}(\text{CH}_3)_2(\text{H}_2\text{O})_2\}_3(\beta\text{-XW}_9\text{O}_{33})]^{3-}$ (X = As^{III}, **1**; Sb^{III}, **2**); the balls represent tungsten (black), tin (diagonally hatched), arsenic/antimony (crosshatched), oxygen (white with shadow), carbon (black) and hydrogen (small white); water molecules are shown as white balls

Solution NMR spectroscopy is the most elegant technique to prove the existence of **1** and **2** in solution. It is well-known that NMR of the addenda atoms (in this case tungsten) is the most sensitive analytical tool to obtain structural information of polyoxoanions in solution. Compounds **1a** and **2a** are ideal for a multinuclear NMR study because they are diamagnetic and contain several NMR-active, spin 1/2 nuclei. Therefore we performed ¹⁸³W, ¹¹⁹Sn, ¹H and ¹³C NMR studies on (a) freshly synthesized solutions of **1a** and **2a** (see Exp. Sect.) and (b) solid **1a** and **2a** redissolved in water. Interestingly we obtained exactly the same NMR results in both cases.

The ¹⁸³W NMR spectrum shows five peaks (intensity ratios 2:1:2:2:2) for **1a** at $\delta = -130.5, -135.2, -138.1,$

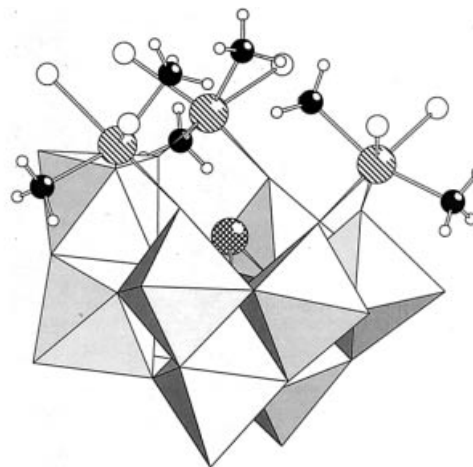


Figure 4. Combined polyhedral/ball-and-stick representation of **1** and **2**; the code is the same as in Figure 3

–142.5 and –146.2 ppm and for **2a** at $\delta = -108.1, -117.4, -120.1, -127.1$ and -134.7 ppm (see Figure 5). The latter spectrum shows an additional, very small peak at $\delta = -124.6$ ppm for which we do not yet have a good explanation. We also recorded a ¹¹⁹Sn NMR spectrum and observed two peaks with an intensity ratio of 1:2 at $\delta = -175.9, -200.0$ ppm (**1a**) and $\delta = -164.6, -205.2$ ppm (**2a**), respectively (see Figure 6). Interestingly both signals for **1a** are somewhat broader than those for **2a**. The ¹³C NMR spectrum shows only one peak for **1a** at $\delta = 8.5$ ppm and for **2a** at $\delta = 8.7$ ppm. As expected, the ¹H NMR spectrum also shows only one peak at $\delta = 4.7$ ppm for **1a** and **2a**. All these results indicate that a species with C_s symmetry is present in solution and prove the existence of the discrete, monomeric polyanions **1** and **2**. Furthermore, the above NMR spectra do not change for several months; indicating that the dimethyltin groups are tightly bound to the tungsten-oxo fragment.

Polyoxoanions **1** and **2** were synthesized by heating an aqueous solution containing dimethyltin dichloride and Na₉[α -XW₉O₃₃] (X = As^{III}, Sb^{III}) in the appropriate stoichiometric ratio (3:1) in an aqueous, acidic medium (pH 3). From this solution the polymeric materials **1a** and **2a** were formed upon crystallization and both products could be isolated in good yield (see Exp. Sect.).

Interestingly, formation of **1** and **2** is accompanied by the isomerization ($\alpha\text{-XW}_9\text{O}_{33} \rightarrow \beta\text{-XW}_9\text{O}_{33}$) (X = As, Sb), and it is likely that steric interactions of the methyl groups do not allow formation of the hypothetical trisubstituted α -derivative $[\{\text{Sn}(\text{CH}_3)_2(\text{H}_2\text{O})_2\}_3(\alpha\text{-XW}_9\text{O}_{33})]^{3-}$ (X = As^{III}, Sb^{III}). More precisely, the three “internal” methyl groups would come very close to each other if they were grafted onto a (α -AsW₉O₃₃) or (α -SbW₉O₃₃) fragment (see Figures 3 and 4). Furthermore the lone pair of electrons on the heteroatom may exhibit a repulsive effect on the internal methyl groups. Rotation of one W₃O₁₃ triad by 60° results in the β -isomer and then all three dimethyltin units can be bound without steric hindrance, resulting in a stable structure. The terminal oxygens of all tin atoms in **1** and **2** are

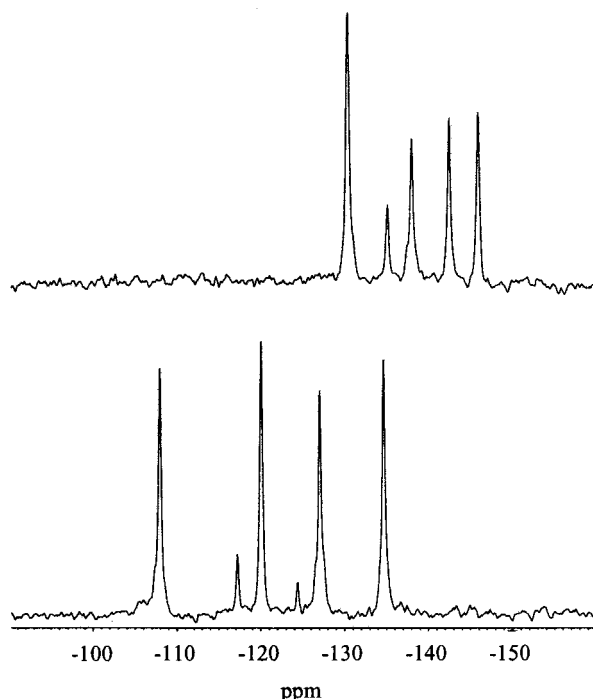


Figure 5. Room-temperature ^{183}W NMR spectra of **1a** (top) and **2a** (bottom) in D_2O

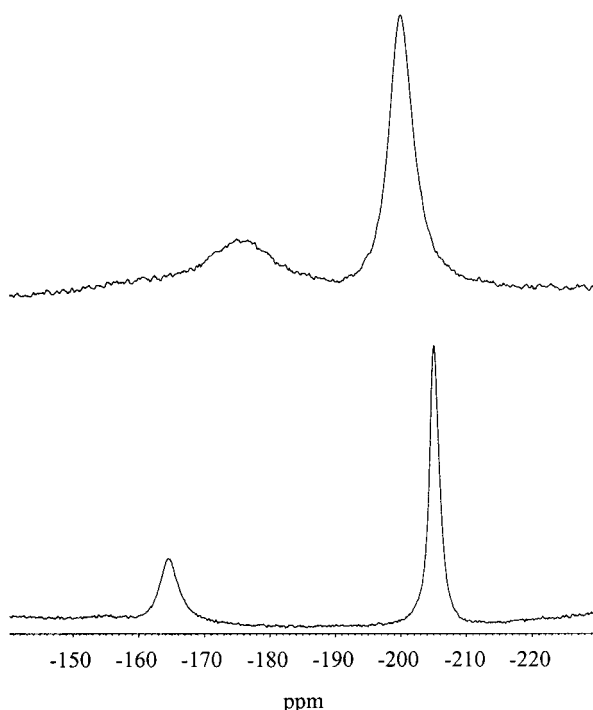


Figure 6. Room-temperature ^{119}Sn NMR spectra of **1a** (top) and **2a** (bottom) in D_2O

almost certainly diprotonated. The presence of labile water ligands explains the tendency of **1** and **2** to polymerize in the solid state.

Conclusions

Our work has shown that diorganotin fragments can be incorporated into polyoxotungstates. Polyanions **1** and **2** represent (a) novel examples of hybrid organic-inorganic polyoxoanions, (b) the first examples of diorganotin-substituted polyoxoanions, (c) the first monomeric organotin derivatives of lone-pair-containing polyoxoanions, and (d) the first organotin derivatives of $[\beta\text{-AsW}_9\text{O}_{33}]^{9-}$ and $[\beta\text{-SbW}_9\text{O}_{33}]^{9-}$. The compounds presented here are rare examples of discrete polyoxoanions which polymerize upon crystallization, leading to a 2-D structure with inorganic and organic surface regions. We plan to prepare derivatives of polyanions **1** and **2** by attaching organic functional groups (e.g. COOH , NH_2 , OH , SH) and chiral subunits (e.g. amino acids) to the organotin fragments. Such species would be of major interest for catalytic and medicinal applications (e.g. stabilization of metal nanoparticles, interaction with biomolecules).

Currently we investigate the possibility of grafting diorganotin units on other lacunary polyoxotungstates.

Experimental Section

The lacunary precursors $\text{Na}_9[\alpha\text{-AsW}_9\text{O}_{33}]$ and $\text{Na}_9[\alpha\text{-SbW}_9\text{O}_{33}]$ were synthesized according to published procedures and their purity was confirmed by infrared spectroscopy.^[17,20] All other reagents were used as purchased without further purification. All elemental analyses were performed by Kanti Labs Ltd. in Mississauga, Canada. The IR spectra were recorded on a Nicolet Avatar FTIR spectrophotometer in a KBr pellet. All NMR spectra were recorded, on a 400 MHz JEOL ECX instrument. The ^{183}W NMR measurements were performed at 16.656 MHz in 10 mm tubes and the ^{119}Sn , ^{13}C , and ^1H spectra were recorded in 5 mm tubes at 149.081, 100.525 and 399.782 MHz, respectively. The chemical shifts for unbound dimethyltin dichloride at pH 3 are at $\delta = -243.7$ ppm (^{119}Sn), 12.2 ppm (^{13}C) and 0.84 ppm (^1H).

(CsNa₂{[Sn(CH₃)₂]₃(H₂O)₄($\beta\text{-AsW}_9\text{O}_{33}$)]·7H₂O)_∞ (1a**):** $\text{Sn}(\text{CH}_3)_2\text{Cl}_2$ (0.58 g, 2.64 mmol) was dissolved in 40 mL of H_2O and then $\text{Na}_9[\alpha\text{-AsW}_9\text{O}_{33}]$ (2.00 g, 0.80 mmol) was added. This solution (pH 3) was heated to 80 °C for 1 h and then cooled to room temperature and filtered. A few drops of 0.1 M CsCl were added and then the solution was allowed to evaporate in an open beaker at room temperature. After 1–2 days a white crystalline product started to appear. Evaporation was allowed to continue until the solvent level had approached the solid product, which was filtered off and air-dried. A total of 1.9 g (yield 76%) of crystalline product was obtained. **1a** (3081.0): calcd. Cs 4.3, Na 1.5 Sn 11.6, As 2.4, W 53.7; found Cs 4.0, Na 1.8, Sn 10.9, As 2.1, W 54.0. IR for **1a** (KBr disk): $\tilde{\nu} = 954, 909, 870, 829, 760, 727, 688, 518, 476, 430 \text{ cm}^{-1}$. NMR (D_2O , 293 K) for **1a**: ^{183}W (relative intensities in parentheses): $\delta = -130.5$ (2), -135.2 (1), -138.1 (2), -142.5 (2), -146.2 (2) ppm. ^{119}Sn : $\delta = -175.9$ (1), -200.0 (2) ppm. ^{13}C : $\delta = 8.5$ ppm. ^1H : $\delta = 4.7$ ppm.

Table 1. Crystal data and structure refinement for **1a** and **2a**

	1a	2a
Formula	C ₆ H ₄₀ AsCsNa ₂ O ₄₄ Sn ₃ W ₉	C ₆ H ₄₀ CsNa ₂ O ₄₄ SbSn ₃ W ₉
Mol. wt. (g/mol)	3081.0	3127.9
Crystal color	colorless	colorless
Crystal system	orthorhombic	orthorhombic
Crystal size (mm ³)	0.10 × 0.06 × 0.02	0.11 × 0.06 × 0.04
Space group (No.)	<i>Pna</i> 2 ₁ (33)	<i>Pna</i> 2 ₁ (33)
<i>a</i> (Å)	26.118(2)	26.118(2)
<i>b</i> (Å)	16.064(1)	16.064(1)
<i>c</i> (Å)	13.776(1)	13.776(1)
Volume (Å ³)	5779.4(7)	5779.4(7)
<i>Z</i>	1	1
<i>D</i> _{calcd} (Mg·m ⁻³)	3.561	3.672
Abs. coeff. (mm ⁻¹)	20.548	20.595
Reflections (unique)	14373	14370
Reflections (obsd.)	11413	12214
<i>R</i> (<i>F</i> _o) ^[a]	0.068	0.052
<i>R</i> _w (<i>F</i> _o) ^[b]	0.1401	0.1078
Diff. peak (e·Å ⁻³)	5.248	2.985
Diff. hole (e·Å ⁻³)	−5.107	−3.762

^[a] $R = \sum ||F_o| - |F_c|| / \sum |F_o|$. ^[b] $R_w = [\sum w(F_o^2 - F_c^2)^2 / \sum w(F_o^2)]^{1/2}$.

(CsNa₂[{Sn(CH₃)₂]₃(H₂O)₄(β-SbW₉O₃₃)]·7H₂O)_∞ (**2a**): The synthesis was identical to that of **1a**, with the exception that 2.00 g (0.80 mmol) of Na₉[α-SbW₉O₃₃] was used instead of Na₉[α-AsW₉O₃₃]. A total of 2.0 g (yield 79%) of crystalline product was obtained. **2a** (3127.9): calcd. Cs 4.2, Na 1.5, Sn 11.4, Sb 3.9, W 52.9; found Cs 3.9, Na 1.3, Sn 11.2, Sb 3.8, W 53.4. IR of **2a** (KBr disk): $\tilde{\nu} = 951, 865, 820, 747, 677, 520, 473, 457, 422 \text{ cm}^{-1}$. NMR (D₂O, 293 K) for **2a**: ¹⁸³W: (relative intensities in parenthesis): $\delta = -108.1$ (2), -117.4 (1), -120.1 (2), -127.1 (2), -134.7 (2) ppm. ¹¹⁹Sn: $\delta = -164.6$ (1), -205.2 (2) ppm. ¹³C: $\delta = 8.7$ ppm. ¹H: $\delta = 4.7$ ppm.

X-ray Crystallography: Crystals of **1a** and **2a** were mounted on a glass fiber for indexing and intensity data collection at 173 K on a Bruker D8 SMART APEX CCD single-crystal diffractometer using Mo-*K*_α radiation ($\lambda = 0.71073 \text{ Å}$). Direct methods were used to solve the structure and to locate the heavy atoms (SHELXS-97). The remaining atoms were found from successive difference maps (SHELXL-97). Routine Lorentz and polarization corrections were applied and an absorption correction was performed using the SADABS program.^[21] Crystal data and structure refinement details for **1a** and **2a** are summarized in Table 1.

CCDC-221555 (for **1a**) and -221556 (for **2a**) contain the supplementary crystallographic data for this paper. These data can be obtained free of charge at www.ccdc.cam.ac.uk/conts/retrieving.html [or from the Cambridge Crystallographic Data Centre, 12 Union Road, Cambridge CB2 1EZ, UK; Fax: (internat.) + 44-1223-336-0333; E-mail: deposit@ccdc.cam.ac.uk].

Acknowledgments

U. K. thanks the International University Bremen for research support. U. K. also highly appreciates that the Florida State University Chemistry Department (USA) allowed him unlimited access to the single-crystal X-ray diffractometer. Figure 1–4 were generated by Diamond Version 2.1e (copyright Crystal Impact GbR).

- [1] *Polyoxometalate Chemistry for Nano-Composite Design* (Eds.: T. Yamase, M. T. Pope), Kluwer, Dordrecht, **2002**.
- [2] *Polyoxometalate Chemistry: From Topology via Self-Assembly to Applications* (Eds.: M. T. Pope, A. Müller), Kluwer, Dordrecht, **2001**.
- [3] *Chemical Reviews, Polyoxometalates* (Ed.: C. Hill), **1998**.
- [4] *Polyoxometalates: from Platonic Solids to Anti Retroviral Activity* (Eds.: M. T. Pope, A. Müller), Kluwer, Dordrecht, **1994**.
- [5] M. T. Pope, A. Müller, *Angew. Chem.* **1991**, *103*, 56–70; *Angew. Chem. Int. Ed. Engl.* **1991**, *30*, 34–48.
- [6] M. T. Pope, *Heteropoly- and Isopoly-Oxometalates*, Springer, Berlin, **1983**.
- [7] J. Berzelius, *Pogg. Ann.* **1826**, *6*, 369.
- [8] [8a] J. F. Keggin, *Nature* **1933**, *131*, 908–909. [8b] J. F. Keggin, *Proc. Roy. Soc., A* **1934**, *144*, 75–77.
- [9] D. A. Judd, J. H. Nettles, N. Nevins, J. P. Snyder, D. C. Liotta, J. Tang, J. Ermolieff, R. F. Schinazi, C. L. Hill, *J. Am. Chem. Soc.* **2001**, *123*, 886–897.
- [10] [10a] F. B. Xin, M. T. Pope, *Organometallics* **1994**, *13*, 4881–4886. [10b] F. B. Xin, M. T. Pope, G. J. Long, U. Russo, *Inorg. Chem.* **1996**, *35*, 1207–1213. [10c] F. B. Xin, M. T. Pope, *Inorg. Chem.* **1996**, *35*, 5693–5695. [10d] G. Sazani, M. H. Dickman, M. T. Pope, *Inorg. Chem.* **2000**, *39*, 939–943.
- [11] [11a] Q. H. Yang, H. C. Dai, J. F. Liu, *Transition Metal Chem.* **1998**, *23*, 93–95. [11b] X. H. Wang, H. C. Dai, J. F. Liu, *Polyhedron* **1999**, *18*, 2293–2300. [11c] X. H. Wang, H. C. Dai, J. F. Liu, *Transition Metal Chem.* **1999**, *24*, 600–604. [11d] X. H. Wang, J. F. Liu, *J. Coord. Chem.* **2000**, *51*, 73–82. [11e] X. H. Wang, J. T. Liu, R. C. Zhang, B. Li, J. F. Liu, *Main Group Met. Chem.* **2002**, *25*, 535–539.
- [12] S. Bareyt, S. Piligkos, B. Hasenknopf, P. Gouzerh, E. Lacote, S. Thorimbert, M. Malacria, *Angew. Chem.* **2003**, *115*, 3526–3528; *Angew. Chem. Int. Ed.* **2003**, *42*, 3404–3406.
- [13] M. Rusu, A. R. Tomsa, D. Rusu, I. Haiduc, *Synth. React. Inorg. Met.-Org. Chem.* **1999**, *29*, 951–965.
- [14] [14a] B. Krebs, B. Lettmann, H. Pohlmann, R. Frohlich, Z. Kristallogr. **1991**, *196*, 231–241. [14b] M. Rusu, L. Muresan, A. R. Tomsa, D. Rusu, G. Marcu, *Synth. React. Inorg. Met.-Org.*

- Chem.* **2000**, *30*, 499–511. ^[14c] G. Kastner, H. Reuter, *J. Organomet. Chem.* **2000**, *598*, 381–386. ^[14d] G. Kastner, H. Reuter, *Main Group Met. Chem.* **2000**, *23*, 383–388.
- ^[15] I. D. Brown, D. Altermatt, *Acta Crystallogr., Sect. B* **1985**, *41*, 244–247.
- ^[16] U. Kortz, M. G. Savelieff, B. S. Bassil, B. Keita, L. Nadjjo, *Inorg. Chem.* **2002**, *41*, 783–789.
- ^[17] M. Bösing, I. Loose, H. Pohlmann, B. Krebs, *Chem. Eur. J.* **1997**, *3*, 1232–1237.
- ^[18] U. Kortz, M. G. Savelieff, B. S. Bassil, M. H. Dickman, *Angew. Chem.* **2001**, *113*, 3488–3491; *Angew. Chem. Int. Ed.* **2001**, *40*, 3384–3386.
- ^[19] This conclusion is further supported by a crystal structure which we obtained during the reviewing period of this manuscript. Interaction of $\text{Sn}(\text{CH}_3)_2\text{Cl}_2$ with the well-known $\text{K}_{14}[\text{As}_2\text{W}_{19}\text{O}_{67}(\text{H}_2\text{O})]$ in aqueous solution at pH 3 resulted in crystals that are composed of discrete polyanions **1** rather than the 2-D material **1a**.
- ^[20] C. Tourné, A. Revel, G. Tourné, M. C. R. Vendrell, *Acad. Sc. Paris, Ser. C* **1973**, *277*, 643–645.
- ^[21] G. M. Sheldrick, SADABS, University of Göttingen, **1996**.

Received January 23, 2004

Early View Article

Published Online April 28, 2004